INTERNATIONAL JOURNAL OF CLIMATOLOGY
Int. J. Climatol. **28**: 205–217 (2008)
Published online 29 May 2007 in Wiley InterScience
(www.interscience.wiley.com) DOI: 10.1002/joc.1518

RMetS
ROYAL METEOROLOGICAL SOCIETY

Cloud-radiative impacts on the tropical Indian Ocean associated with the evolution of 'monsoon breaks'

Basanta Kumar Samala and R. Krishnan*
Climate and Global Modelling Division, Indian Institute of Tropical Meteorology, Pashan, NCL Post, Pune 411008, India

ABSTRACT: A detailed diagnostic analysis of a suite of observed datasets was carried out with a view to understand the importance of cloud-radiative effects on the evolution of prolonged 'monsoon breaks' over the Indian region. The study particularly focuses on the role of clouds in affecting the sub-seasonal/intra-seasonal variability of sea surface temperature (SST) and atmospheric convection in the equatorial and south-eastern tropical Indian Ocean (SETIO) during monsoon-break transitions. A characteristic feature of the monsoon-break evolution is the appearance of suppressed convection over the SETIO region nearly 7–10 days prior to the commencement of a break spell over India. It is seen from the present analysis that the lack of cloud cover over the SETIO during the 'pre-break' phase leads to significant warming of the tropical Indian Ocean due to strong solar insolation at the surface. During the 'pre-break' phase, the net cloud-radiative forcing (NETCRF) at the surface is found to be typically around -30 Wm^{-2} and the mean SST in the SETIO is about 29.3 °C. Following the transition to a monsoon-break phase, the cloud amount increases by about 25% over the SETIO region in association with intensified convection. The NETCRF at the surface over the SETIO averaged during the 'break' phase is found to be about -60 Wm^{-2} (i.e. a change of about -30 Wm^{-2} from the 'pre-break' phase). Consistent with the above change in the NETCRF, the SST in the SETIO shows a cooling of about 0.7 °C, although the mean SSTs during the 'break' phase remain as high as 28.6 °C. On the basis of the findings from this study, it is suggested that the SST warming during the 'pre-break' phase plays a key role in maintaining high SST and allows sustained convection to occur over the SETIO during prolonged monsoon breaks. Copyright © 2007 Royal Meteorological Society

KEY WORDS cloud-radiative forcing; monsoon breaks; Indian Ocean

Received 10 June 2006; Revised 3 February 2007; Accepted 3 February 2007

1. Introduction

Clouds play a major role in the energy balance of the Earth's climate system. They exert both a cooling effect by reflecting sunlight back into space and a warming effect by trapping the heat emitted from the surface. For understanding the role of clouds in the climate system, the term 'cloud radiative forcing (CRF)' is a useful concept that provides a measure of how much clouds can modify the net radiation, at wavelengths ranging from 0.3 to 100 μm of the Earth system. Regions of positive CRF indicate areas where clouds act to increase the net energy into the Earth system, while areas of negative CRF signify regions where clouds act to decrease the net energy into the Earth system.

The Earth Radiation Budget Experiment (ERBE) was the first satellite experiment that provided observational estimates of changes in the longwave and shortwave radiative fluxes at the top of the atmosphere due to clouds (Ramanathan *et al*., 1989; Harrison *et al*., 1990; Kiehl and Ramanathan, 1990, Stephens and Greenwald, 1991; Hartmann *et al*., 1992 and others). The ERBE data revealed that changes in the shortwave and longwave fluxes due to the presence of deep clouds over the tropics were nearly of the same magnitude but opposite in sign (Kiehl and Ramanathan, 1990). A near cancellation between the shortwave CRF and longwave CRF in the equatorial Pacific was noted by Kiehl (1994). However, there are regional peculiarities wherein the shortwave and longwave components of CRF at the top of atmosphere (TOA) may not always cancel. For example, Rajeevan and Srinivasan (2000) showed that the widespread coverage of a large amount of high clouds with large optical depths over the Asian summer monsoon region gives rise to a large negative net cloud-radiative forcing (NETCRF) during the June–September months. In a more recent study, Sathiyamoorthy *et al*. (2004) pointed out that the spreading of cloud tops by the strong easterly winds in the upper troposphere can increase the high-cloud amount over the Asian monsoon region during the northern summer.

This paper investigates the importance of cloud-radiative effects that operate on sub-seasonal/intra-seasonal timescales over the tropical Indian Ocean and monsoon environment. The motivation for this study stems due to the occurrence of substantial variations in the regional convective activity in association with the summer monsoon intra-seasonal variability (Goswami, 2005; Waliser, 2005). On this timescale, the fluctuations

* Correspondence to: R. Krishnan, Climate and Global Modelling Division, Indian Institute of Tropical Meteorology, Pashan, NCL Post, Pune 411008, India. E-mail: krish@tropmet.res.in

of monsoon precipitation over the Indian landmass are characterized by periods of enhanced and reduced rainfall – which are commonly referred to as 'active' and 'break' phases of the monsoon (Ramamurthy, 1969; Krishnamurti and Bhalme, 1976; Yasunari, 1979; Sikka and Gadgil, 1980; Krishnamurti and Subrahmanyam, 1982; Singh and Kripalani, 1985; Hartmann and Michelsen, 1989). Prolonged breaks in the monsoon rainfall often result in droughts, which produce adverse socio-economic impacts in the region (Sikka, 1999). While monsoon breaks are associated with suppression of rains over the Indian landmass, it has been known that convection generally intensifies over the near-equatorial Indian Ocean during break periods (e.g. Yasunari, 1979; Sikka and Gadgil, 1980; Lau and Chan, 1986; Krishnan *et al*., 2000; Annamalai and Slingo, 2001 and Krishnan *et al*., 2006).

For example, the extended monsoon break during July 2002, which resulted in a severe drought, is a good case to illustrate this point. The 2002 monsoon drought has been explored by several investigators from different viewpoints (e.g. Fasullo, 2005; Gadgil *et al*., 2005; Kumar and Krishnan, 2005; Krishnan *et al*., 2006; Saith and Slingo, 2006). The mean climatological conditions for July and the anomalous conditions during July 2002 are depicted in Figure 1. The major weakening of the southwest monsoon flow and the rainfall reduction during July 2002 are strikingly evident from the large negative anomalies of precipitation and low-level anti-cyclonic wind anomalies over India (Figure 1(b)). In addition, the anomalous enhancement of rainfall over the equatorial and south-eastern tropical Indian Ocean (SETIO) region during 2002 is an important point to be noted.

The mean climatology of the total cloud and high cloud amounts for July, based on the International Satellite Cloud Climatology Project (ISCCP) dataset (Rossow and Schiffer, 1999), are shown in Figure 1(c) and Figure 1(e) respectively. It can be seen that the climatological total cloud cover over Bay of Bengal and the equatorial eastern Indian Ocean during July is dominated by high clouds. Studies have shown that the surface radiative budget over the equatorial eastern Indian Ocean is largely influenced by high clouds (eg. Fu *et al*., 1996; Rajeevan, 2001). Also, it can be noticed from Figure 1(e) that the climatological high cloud cover is small over the western Arabian Sea off the coasts of Somalia and Arabia. In fact, earlier studies have reported that the contribution of high clouds to the total cloud cover is small over the colder oceanic regions associated with upwelling – e.g. the western Arabian Sea; the subtropical regions of south-eastern Pacific and Atlantic (Fu *et al*., 1996). The anomalies of total cloud and high cloud cover during July 2002 are shown in Figure 1(d) and Figure 1(f) respectively. The cloudiness anomalies during July 2002 depict a pattern of decreased cloudiness over the Indian landmass and increased cloudiness over the SETIO region consistent with that of the rainfall anomalies. In particular, the increased cloudiness over the SETIO during July 2002 was primarily due to high clouds (Figure 1(f)). Also, while the high cloud cover was enhanced over the western Arabian Sea off the Somali Coast during July 2002 (Figure 1(f)), the low clouds were greatly diminished over this region as evident from the negative anomalies of the total cloud cover (Figure 1(d)).

Given the nature of anomalous convection over the SETIO during monsoon breaks, a question that arises is the possible role of cloud-radiative effects in preconditioning the tropical Indian Ocean during the evolution of prolonged monsoon breaks. This issue assumes significance because it provides a basis for understanding the long-lasting nature of convective anomalies over the SETIO region. Here, we particularly focus on extended monsoon – breaks, which are longer than 2 weeks. It is well recognized that air–sea exchanges on intraseasonal timescales in the tropical Indian Ocean give rise to significant fluctuations of sea surface temperature (SST) and heat fluxes at the ocean–atmosphere interface (Rao, 1987; Krishnamurti *et al*., 1988; Bhat *et al*., 2001; Sengupta *et al*., 2001; Sengupta and Ravichandran, 2001; Veechi and Harrison, 2002). Earlier studies have reported anomalous warming of SST preceding a convection maximum in association with positive shortwave and latent heat flux anomalies into the surface (e.g. Hendon and Glick, 1997; Shinoda *et al*., 1998; Woolnough *et al*., 2000). These investigations suggest that spatially coherent SST anomalies, with an amplitude of about 0.3–0.4 °C, develop in the Indian Ocean and propagate eastward along with the large-scale convective anomaly, but with a lag of nearly 10–15 days. Coincident with the convective maximum, the decrease in the shortwave flux and increase in the evaporation from the surface are known to cool SST following the development of convection (Woolnough *et al*., 2000). Coupled model simulations indicate that positive (negative) SST fluctuations in the Bay of Bengal are highly correlated with more (less) precipitation with a lead time of more than a week (Fu *et al*., 2003; Fu and Wang, 2004). Since monsoon-break transitions are accompanied by significant convection changes over the SETIO (e.g. Krishnan *et al*., 2000), it would be worthwhile to examine if cloud-radiative effects can modulate the variability of SST in the SETIO during the evolution of prolonged monsoon breaks. This study is based on analyses of satellite observations of shortwave and longwave CRF at the TOA; radiative flux products at the surface, SST and related parameters. The datasets used in the present study are described in the following section.

2. Data

Monthly shortwave and longwave fluxes at the TOA based on radiometric measurements from the Clouds and the Earth's Radiant Energy System (CERES) mission for the period March 2000 to February 2003 (Wielicki *et al*., 1996) are employed to understand the CRF at the TOA during the evolution of the prolonged monsoon break of July 2002. The total

DOI: 10.1002/joc

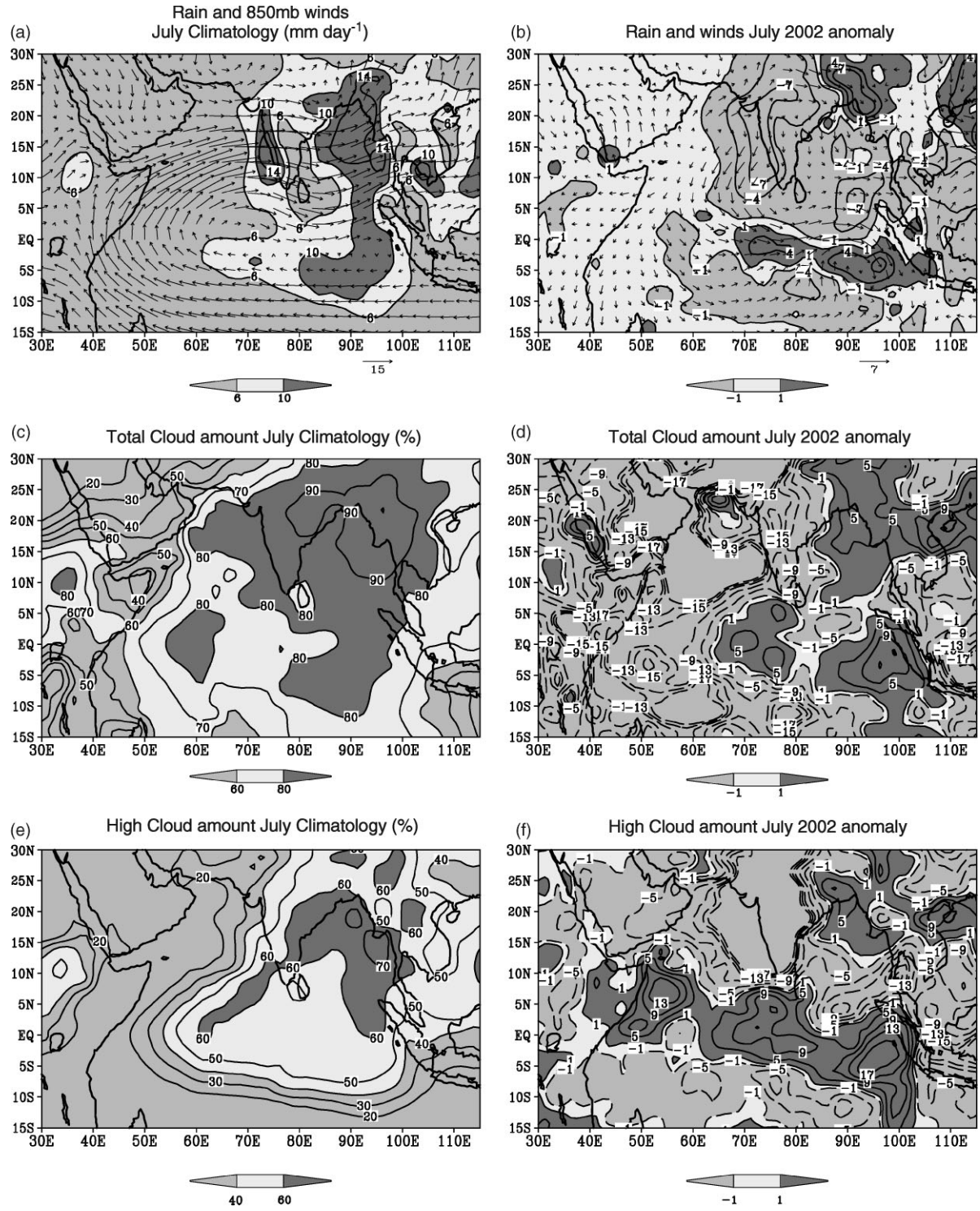

Figure 1. **(a)** Mean climatological rainfall (mm day^{-1}) from CMAP dataset and 850 hPa winds (ms^{-1}) from NCEP reanalysis for July. Notice the climatological precipitation maxima over the head Bay of Bengal, northeast India and the west coast of India. A secondary rainfall maximum is seen over the SETIO region. The low-level winds show the southwest monsoon circulation with strong cross-equatorial flow from the Indian Ocean. **(b)** Rainfall and wind anomaly during July 2002 **(c)** Climatology of total cloud amount (%) for July from ISCCP dataset **(d)** Anomaly of total cloud amount during July 2002 **(e)** Same as (c) except for high clouds **(f)** Same as (d) except for high clouds.

and high clouds used in our analysis are based on the ISCCP D2 dataset (Rossow and Schiffer, 1999) obtained from ftp://isccp.giss.nasa.gov/pub/data/D2Tars. The ISCCP dataset, which is constructed on the basis of infrared and visible radiances obtained from imaging radiometers aboard the international constellation of weather satellites, provides information about global distribution of clouds, their radiative properties, their variations on diurnal, seasonal and inter-annual timescales. The dataset is available from July 1983 onward. The ISCCP D2 version represents a significant improvement over the previous version due to (1) revised radiance

DOI: 10.1002/joc

calibrations for removal of spurious changes in the long-term record, (2) increased cirrus detection sensitivity over land, (3) increased low-level cloud detection sensitivity in polar regions, (4) reduced biases in cirrus cloud properties and (5) increased detail about the variations in cloud properties (Rossow and Schiffer, 1999).

For the CRF at surface, we have examined ISCCP Radflux monthly dataset, in which the shortwave and longwave radiative fluxes are determined on the basis of observations and model calculations (Zhang *et al*., 2004). Besides the monsoon break of July 2002, we have also examined the cloud-radiative effects during other instances of prolonged break spells in the past by analysing the global daily Surface Radiation Budget (SRB) dataset, which is available for the period 1983–1993. The SRB dataset uses information about clouds from ISCCP, TOA clear-sky albedo from ERBE along with TOA radiances and profiles of atmospheric water vapour and temperature, in a model for computing longwave and shortwave radiative properties at the surface (http://eosweb.larc.nasa.gov/PRODOCS/srb). Other datasets used in our analysis are the daily SST in the tropical Indian Ocean based on the TRMM Microwave Imager (TMI) dataset, which is available for the period December 1997–December 2005 (ftp://ftp.ssmi.com/tmi); weekly optimum interpolation sea surface temperature (OISST) dataset derived from *in situ* observations and the NOAA advanced very high resolution radiometer (AVHRR) satellite measurements available since 1981 (http://www.cdc.noaa.gov/cdc/data.noaa.oisst.v2.html) and rainfall from the Climate Prediction Center (CPC) merged analysis of precipitation (CMAP) and atmospheric winds from the National Center for Environmental Prediction (NCEP) reanalysis (http://www.cpc.ncep.noaa.gov/products).

3. CRF and SST variations in the tropical Indian Ocean

3.1. CRF at the TOA

The longwave CRF at the TOA is defined as (LWCRF $= F_{\mathrm{clr}} - F$) where F_{clr} and F are the 'clear-sky' and 'all-sky' longwave radiative fluxes respectively. LWCRF measures the decrease in thermal energy into the space radiated by the atmospheric column due to the presence of clouds and is typically a positive quantity. The shortwave CRF at the TOA is defined as SWCRF (TOA) $= S\,(\alpha_{\mathrm{clr}} - \alpha)$, where S is the monthly incoming solar flux at the top of the atmosphere and α is the total sky albedo of the earth-atmosphere system and α_{clr} is the clear-sky albedo of the Earth's atmosphere system. Basically, SWCRF describes the difference between the clear sky and cloudy sky reflected solar fluxes at TOA. When clouds are present, they reflect more solar energy into space than would clear skies. SWCRF gives a quantitative estimate of this effect and is typically negative. The NETCRF is defined as the sum of SWCRF and LWCRF and the sign depends upon the relative values of LWCRF and SWCRF.

The all-sky and clear-sky shortwave fluxes from CERES measurements during July 2002 are shown in Figure 2(a–b). The corresponding longwave fluxes are shown in Figure 2(c–d). Regions where clear-sky scenes were absent (e.g. the Indo–China region, northeast and northwest India) are indicated by blank areas in Figure 2(b) and (d). Our region of primary interest is the SETIO, where the cloud cover was enhanced during July 2002. It can be seen from Figure 2(a) and (b) that the magnitude of the all-sky shortwave flux over the SETIO was significantly higher than the clear-sky shortwave flux. The all-sky shortwave flux averaged for the region (70 °E–100 °E; 10 °S – Equator) was found to be about 100 Wm^{-2} and the corresponding clear-sky shortwave flux was about 34 Wm^{-2}, so that the SWCRF was around -66 Wm^{-2}. On the other hand, the all-sky longwave flux for the same region was about 220 Wm^{-2} and the clear-sky longwave flux was about 285 Wm^{-2}, so that the LWCRF was nearly 65 Wm^{-2}. The SWCRF and LWCRF at the TOA over the SETIO during July 2002 were nearly of same magnitude but opposite in sign, which is consistent with the ERBE observations (e.g. Kiehl and Ramanathan, 1990; Kiehl, 1994).

The changes in the SWCRF and LWCRF over the SETIO between June and July 2002 can be inferred from Figure 3. It can be seen that the cloud cover over the SETIO was relatively less during June 2002 as compared to July 2002 – the latter period coinciding with intense monsoon-break conditions over the Indian landmass (Figure 3(a–b)). The convective activity over the SETIO basically intensified during July 2002, while it was not as strong in June 2002. Further, it can be seen from Figure 3(c) and (d) that the increased cloud cover over the SETIO during July 2002 was mainly due to high clouds. The SWCRF values averaged over the region (70 °E–100 °E; 10 °S – Equator) were found to be around -57 Wm^{-2} in June 2002 and -66 Wm^{-2} in July 2002 respectively (Figure 3(e) and (f)). The corresponding LWCRF values during June and July 2002 were about $+55$ Wm^{-2} and $+65$ Wm^{-2} respectively (Figure 3(g) and (h)). Basically, the increase in the LWCRF at the TOA from June to July 2002 was more or less compensated by a similar decrease in the SWCRF.

3.2. CRF at the surface

In contrast to the cloud-radiative effects at the TOA, the NETCRF at the surface is known to be primarily determined by changes in the shortwave component; while the longwave effects have a minor contribution (Collins *et al*., 1996). The SWCRF at the surface is computed as the difference between all-sky surface downward SW flux and clear-sky downward SW flux. The SWCRF variations at the surface during 2002, based on ISCCP-FD Radflux dataset, are shown in Figure 4. The SWCRF averaged over the SETIO region was found to be around -60 Wm^{-2} in June 2002, while it was around -100 Wm^{-2} during July 2002. Thus, the change in SWCRF over the SETIO region by nearly -40 Wm^{-2},

DOI: 10.1002/joc

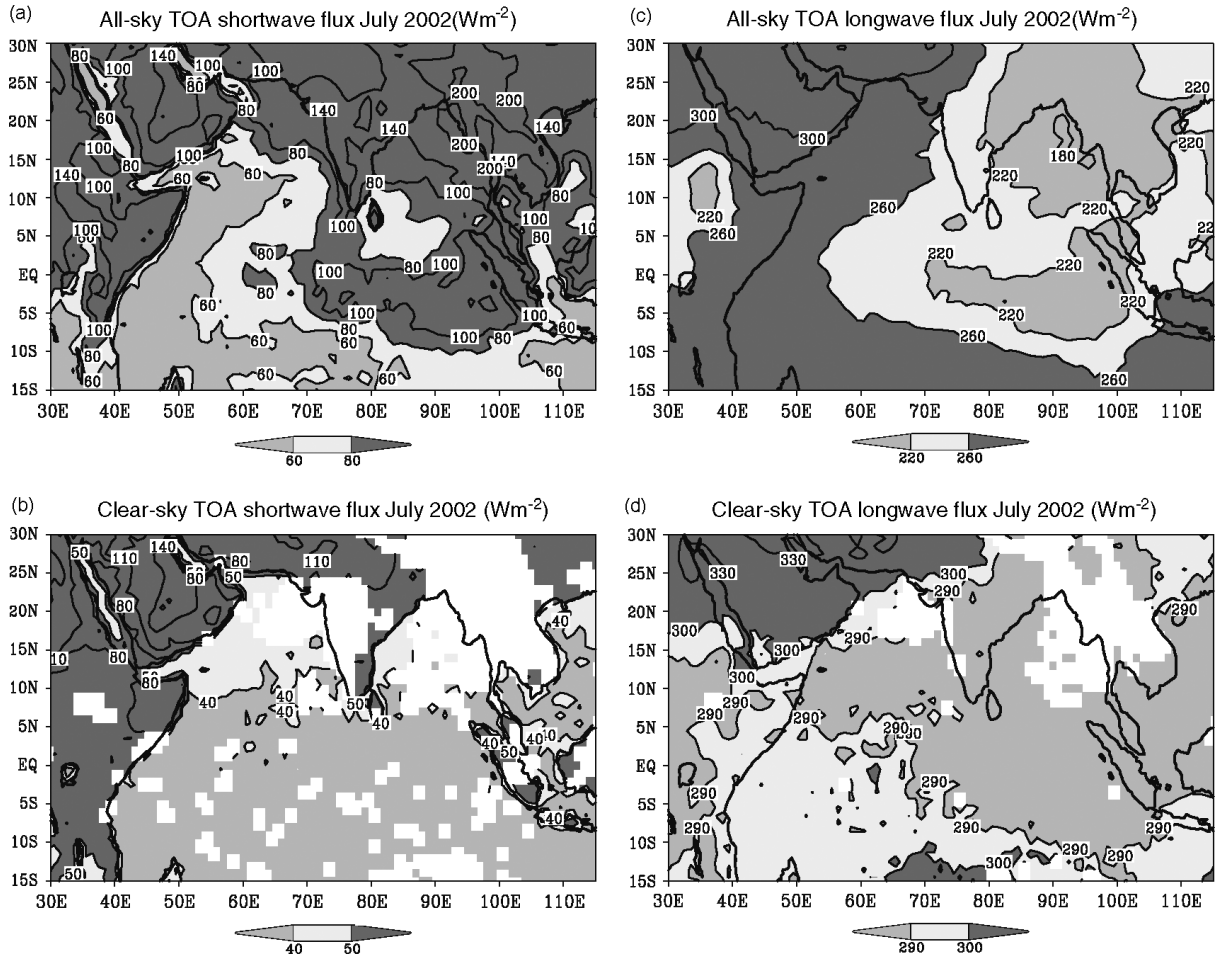

Figure 2. TOA fluxes (Wm^{-2}) for July 2002 from CERES **(a)** All-sky shortwave flux **(b)** Clear-sky shortwave flux **(c)** All-sky longwave flux **(d)** Clear-sky longwave flux.

from June 2002 to July 2002, is consistent with the increase in cloud cover over the region (Figure 4(c)). However, the corresponding change in the LWCRF at surface from June to July 2002 over the SETIO is relatively small as compared to that of the SWCRF (Figure 4(d–f)). This clearly indicates that, it is the shortwave component that dominates the cloud-radiative effects at the surface. In other words, the change of about -40 Wm^{-2} in the SWCRF over the SETIO region, due to increased cloud cover, basically points to a smaller net heat loss from the ocean during June 2002 relative to that of July 2002.

3.3. Intra-seasonal variation of SST in SETIO during 2002

In order to understand the cloud-radiative effects on the intra-seasonal variability of SST in the SETIO during 2002, we examined the daily SST from the TMI dataset – which provides an unprecedented view of tropical SST variability in the presence of atmospheric convection and clouds (Wentz, 1998; Chelton *et al*., 2001; Harrison and Vecchi, 2001). The time series of SST averaged in the SETIO region is shown from June through September 2002 in Figure 5. It can be seen that the SST was higher than 29.3 °C during most of June 2002 and decreased substantially during July and early August of 2002. While the high SST during June 2002 is consistent with relatively less cloud cover over SETIO, it can be seen that the magnitude of SST dropped by more than 1 °C from the beginning of June 2002 to the end of July 2002 (Figure 5). Also, notice that the SST during June 2002 was anomalously warmer than the mean climatological SST by more than 0.5 °C. In addition, it is very important to recognize that the mean SST during July to September 2002 was quite high (>28 °C) in the SETIO. Krishnan *et al*. (2006) have reported that the high SST in the SETIO during 2002 was also associated with an anomalous deepening of the oceanic mixed layer and depression of the thermocline in the region. This issue is discussed in Section 5. The important point here is the occurrence of very high SST in the SETIO during June 2002, indicating a pre-conditioning of the equatorial Indian Ocean prior to the commencement of the prolonged monsoon break during July 2002.

3.4. Surface CRF from SRB dataset (1983–1993)

The results from the 2002 analysis motivated us to examine the CRF at the surface during other instances of monsoon breaks in the past. For this purpose, we have

DOI: 10.1002/joc

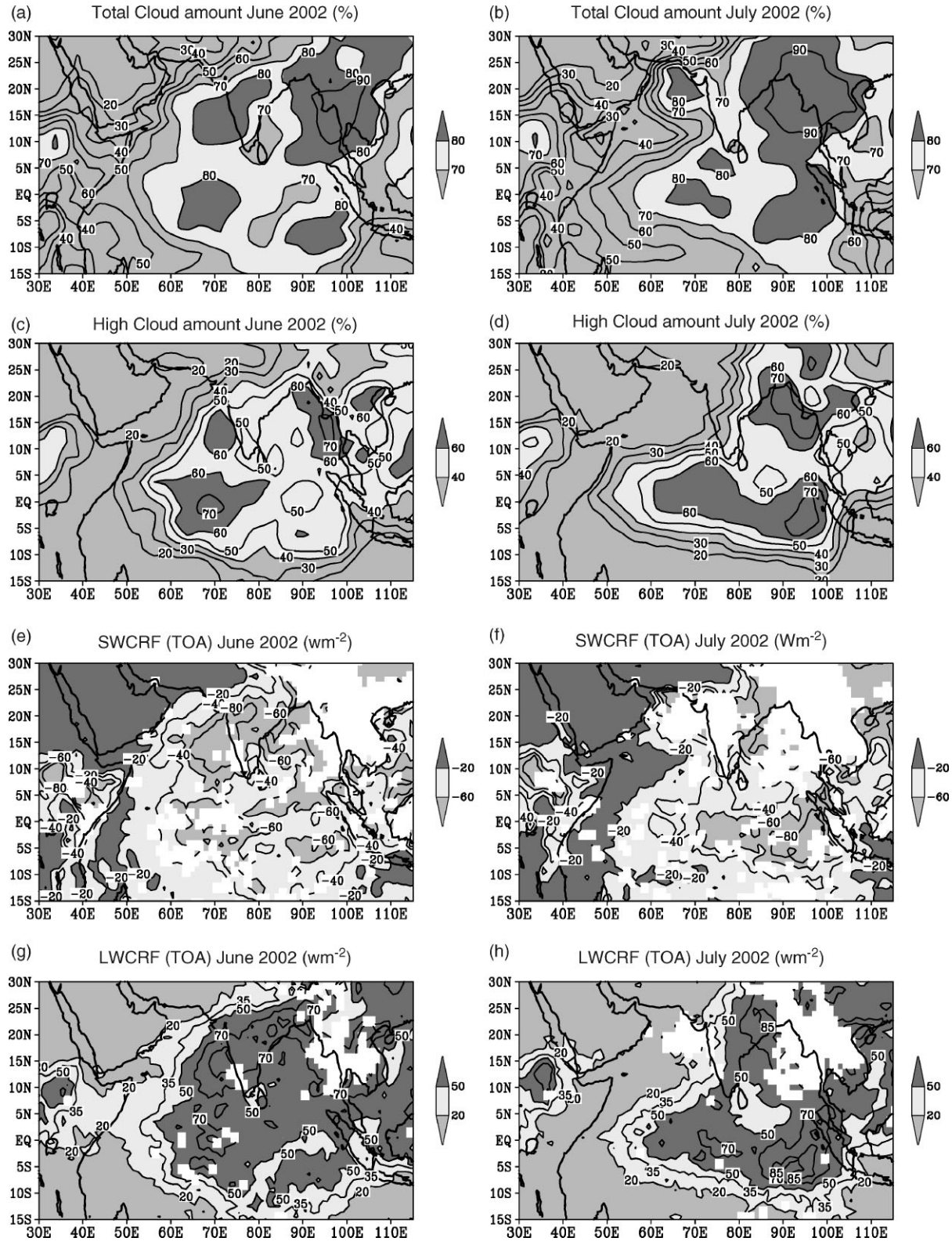

Figure 3. Clouds from ISCCP and CRF at TOA from CERES during June 2002 (left column) and July 2002 (right column) **(a–b)** Total cloud amount (%) **(c–d)** High cloud amount (%) **(e–f)** SWCRF (Wm^{-2}) **(g–h)** LWCRF (Wm^{-2}).

used the SRB daily dataset, which is available from 1983 through 1993. On the basis of the monsoon-break days identified by Krishnan *et al.* (2000), we have considered cases of prolonged monsoon breaks during 1983–1993, which are given in Table I. Figure 6(a) shows the composite of the cloud amount based on the monsoon-break days listed in Table I. The enhanced cloudiness over the SETIO and decreased cloud amount over the Indian landmass brings out the regional contrast in the cloudiness pattern associated with monsoon breaks.

DOI: 10.1002/joc

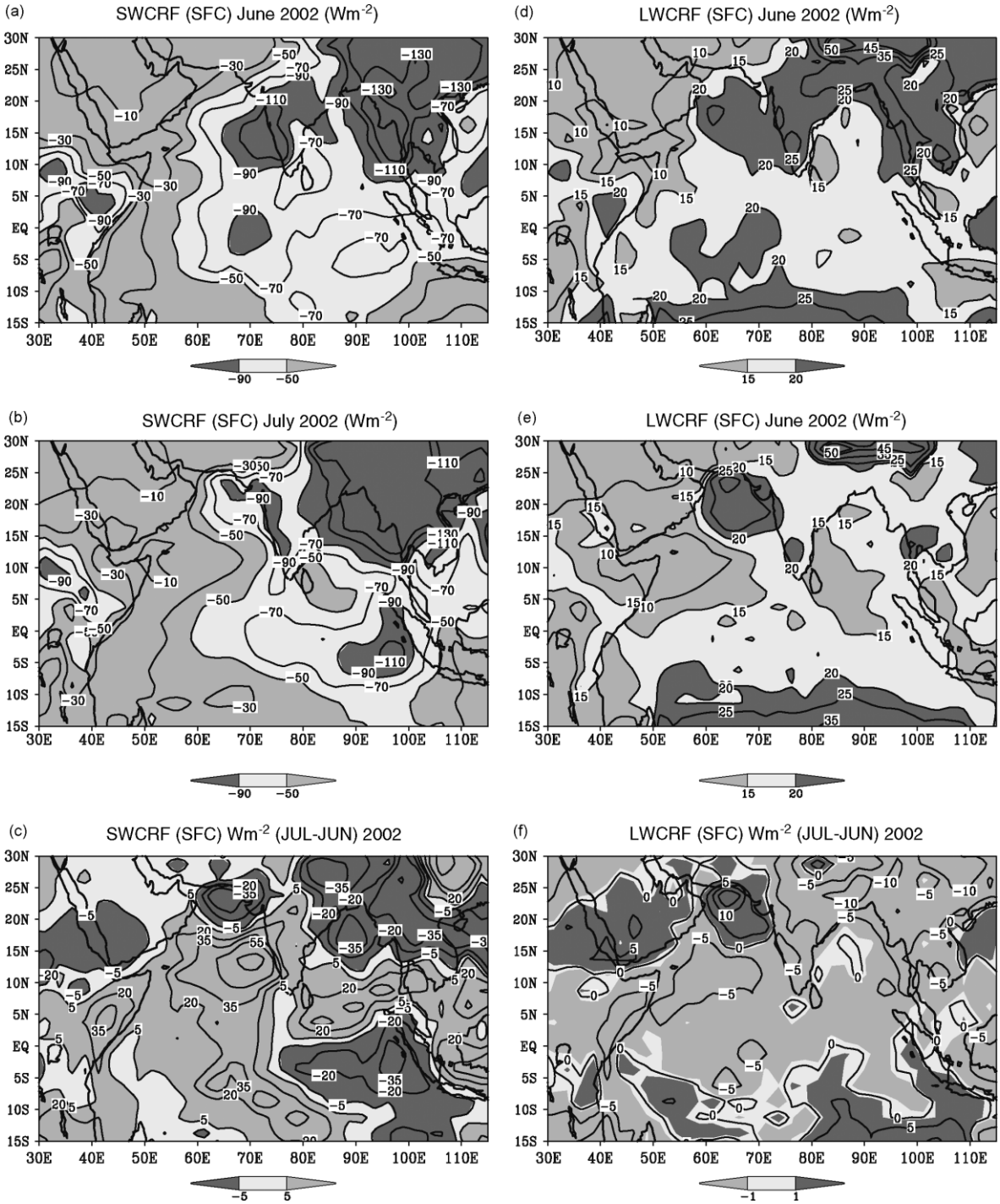

Figure 4. SWCRF (Wm^{-2}) and LWCRF (Wm^{-2}) at surface from ISCCP-FD Radflux dataset **(a)** SWCRF for June 2002 **(b)** SWCRF for July 2002 **(c)** Difference in SWCRF (July minus June, 2002) **(d)** LWCRF during June 2002 **(e)** LWCRF during July 2002 **(f)** Difference in LWCRF (July minus June, 2002).

The enhanced cloud amount over northeast India in Figure 6(a) is a typical feature seen during weak phases of the southwest monsoon that results from a northward shift of the monsoon trough from its normal position (Ramamurthy, 1969; Rao, 1976). The SWCRF at the surface shows negative values of about -110 W m^{-2} over the SETIO region associated with the large cloud amounts (Figure 6(b)). However, the surface LWCRF over the SETIO is relatively small in magnitude ($\sim$25 Wm^{-2}) in the monsoon-break composite (Figure 6(c)).

We now contrast the cloud-radiative effects between 'break' *versus* 'pre-break' phases. The composite of cloud amounts during the pre-break phase is shown in Figure 6(d). The pre-break composite is based on averages over 10 days preceding the commencement of each monsoon break. The well-defined east–west-oriented cloud band across South Asia (Figure 6(d)) indicates a very active phase of the monsoon convective activity over the Indian subcontinent. The enhanced cloudiness is corroborated by the strong negative SWCRF

DOI: 10.1002/joc

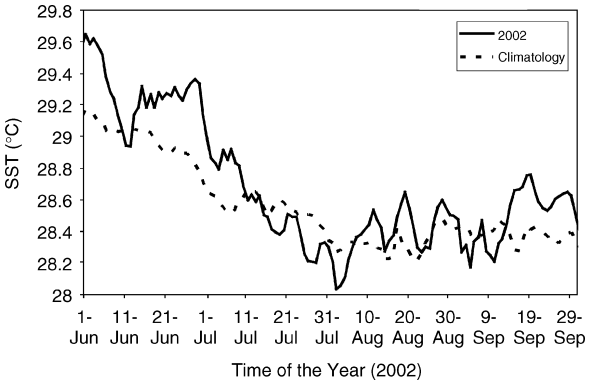

Figure 5. Daily SST averaged for the region (70 °E–100 °E; 10 °S-Equator) from the TMI dataset. The solid line is for 2002 and the dashed line is the climatological mean for the 8-year baseline period (1998–2005). It is important to notice the strong SST warming during June 2002 prior to the monsoon break in July 2002. The SST in the SETIO dropped by nearly 1 °C during the intense monsoon break of July 2002.

Table I. List of prolonged monsoon-break days.[a]

Case	Year	Break period	No. of days
1	1979	12 August–27 August	16
2	1982	24 June–7 July	14
3	1986	20 August–8 September	20
4	1987	14 July–3 August	21
5	1992	25 June–9 July	15
6	2002	3 July–30 July	28
7	2004	19 June–2 July	14

[a] The identification of monsoon-break days is based on the criteria adopted by Krishnan *et al*. (2000) using satellite OLR data. Here, we have considered prolonged break spells, which are longer than 2 weeks. For the SRB dataset, which is available from July 1983 to June 1995, the prolonged break days during 1986, 1987 and 1992 are used in our analysis. Likewise, for the TMI data, which is available since Dec 1997, we have used the prolonged breaks of 2002 and 2004 in our analysis.

over the Indian landmass, Bay of Bengal and Arabian Sea in Figure 6(e). In contrast to the conditions over the subcontinent, the cloud amounts and SWCRF are quite low over the SETIO during the pre-break phase (Figure 6(d), (e)). The LWCRF during the pre-break phase is shown in Figure 6(f). Comparison of Figure 6(e) and (f) shows that the magnitude of LWCRF at the surface is smaller relative to that of the SWCRF, with the latter mainly contributing to the NETCRF at the surface. The change in the cloud amount ('break minus pre-break') is shown in Figure 7(a). While the cloud amount over the Indian region shows a decrease by as much as 25% during the transition from the pre-break phase to the monsoon-break phase, the cloud amount over the SETIO shows an increase of a more or less similar magnitude. The change in NETCRF at the surface (Figure 7(b)) associated with the transition from the pre-break phase to the monsoon-break phase shows positive values (>50 Wm^{-2}) over the Indian landmass and negative values of similar magnitude over the SETIO.

3.5. Daily variation of convection and CRF over India and SETIO

The commencement of a monsoon break over the Indian subcontinent is preceded by significant convection changes over the tropical Indian Ocean, which can be inferred from satellite observations of outgoing longwave radiation (OLR). Krishnan *et al*. (2000) noted the appearance of suppressed convection and high pressure anomalies over the equatorial Indian Ocean nearly 7–10 days prior to the initiation of a monsoon break over India; subsequently, the convectively stable anomalies were found to spread over the eastern Indian Ocean and also extended northward over the Bay of Bengal. Their analysis showed that monsoon breaks tend to be initiated following a rapid west-northwest movement of the dry convectively stable anomalies from the Bay of Bengal into north-central India.

Figure 8(a) shows the time series of OLR anomalies over the Indian landmass (solid line) and SETIO (dashed line) – which have been composited from several cases of extended monsoon breaks (Table I). In Figure 8(a), Day (0) corresponds to the day of monsoon-break initiation. The days preceding Day (0) correspond to the 'pre-break' phase (i.e. Day -10, Day $-9 \ldots$ Day -1); and the days following the initiation of monsoon break (i.e. 'break' phase) are given by (Day $+1 \ldots$ Day $+14$, Day $+15$). It can be seen that, prior to the commencement of monsoon-breaks, above-normal convective activity (i.e. negative OLR anomaly) prevails over the Indian landmass. At this time, convection over the SETIO is subdued as evidenced from the positive OLR anomalies. Following the commencement of the monsoon-break phase, suppressed convection appears over the Indian landmass with positive OLR anomalies as high as $+40$ Wm^{-2}. In contrast, the OLR anomalies over the SETIO show negative values as low as -25 Wm^{-2} during the break phase. The intensification of convective activity over the SETIO can be seen from day $+2$ onward. The out-of-phase variability of convection over the Indian landmass and the SETIO is consistently reflected in the daily evolution of the NETCRF at the surface (Figure 8(b)). The NETCRF at the surface shows a gradual rise over the Indian landmass – with a mean value of about -82 Wm^{-2} during the 'pre-break' phase and about -37 Wm^{-2} during the 'break' phase respectively. In contrast, the NETCRF at the surface over the SETIO region shows a decline as the monsoon break evolves – with a mean value of about -33 Wm^{-2} during the 'pre-break' phase and about -57 Wm^{-2} during the 'break phase respectively.

4. SST changes associated with monsoon-break transitions

The signatures of cloud forcing on the ocean temperature anomalies, associated with monsoon-break transitions, are examined using SST from the OISST as well as the TMI datasets. While the OISST data has a longer temporal coverage from 1981 onward, it is basically a

DOI: 10.1002/joc

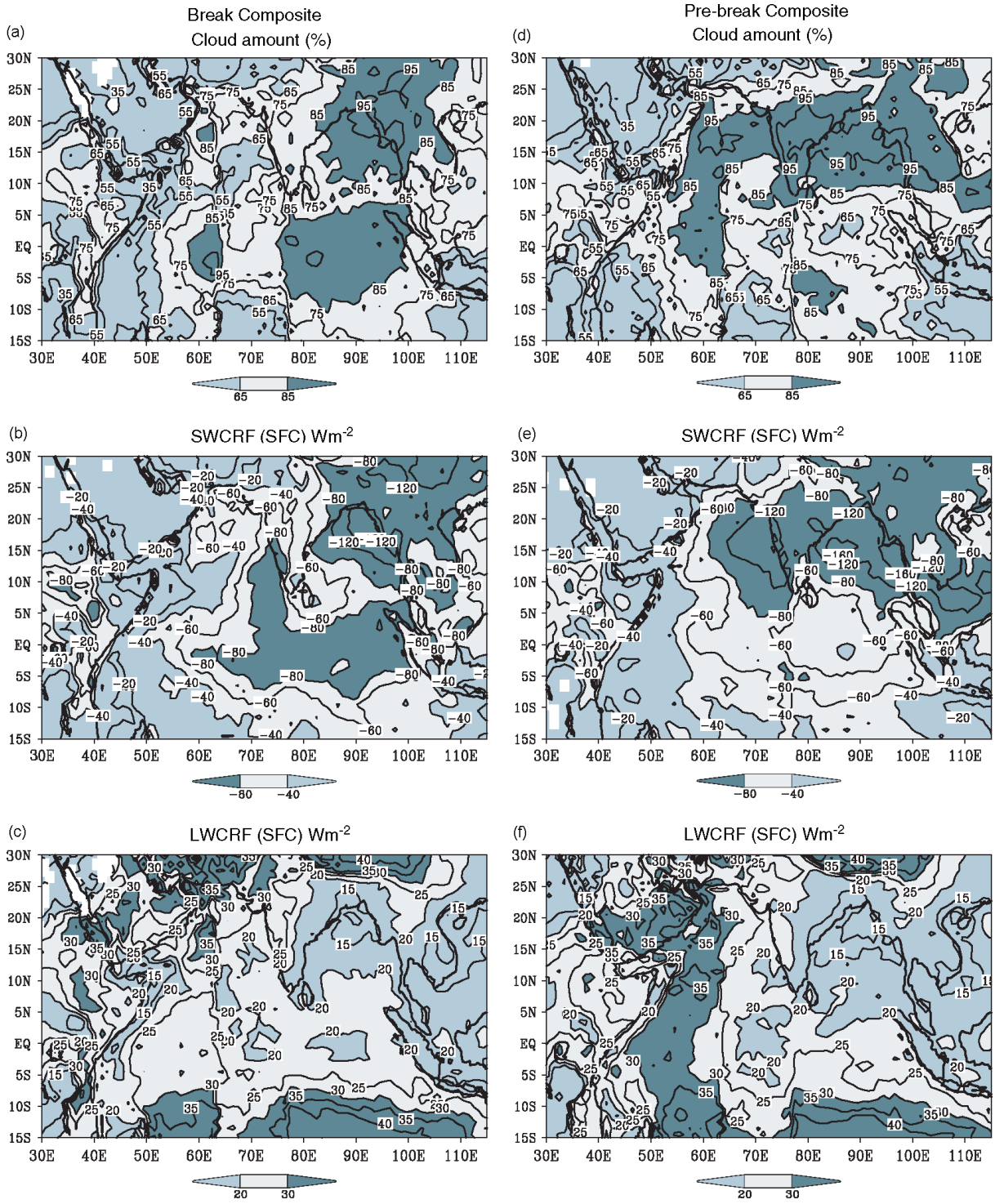

Figure 6. Composites of total cloud amount (%), surface SWCRF (Wm^{-2}) and surface LWCRF (Wm^{-2}) during 'break' and 'pre-break' phases – constructed from the Surface Radiation Budget (SRB) dataset with respect to (w.r.t.) the prolonged monsoon breaks during 1986, 1987 and 1992. The 'break' composites are based on the monsoon-break days given in Table I. The 'pre-break' composites are 10-day averages prior to commencement of each of the break spell. The figures in the left column **(a, c, e)** correspond to the 'break' composites and the figures in the right column **(b, d, f)** correspond to the 'pre-break' composites. This figure is available in colour online at www.interscience.wiley.com/ijoc

weekly SST product. Moreover, since the OISST dataset is derived from AVHRR, the accuracy of SST measurements can be affected due to obstruction by clouds in the field of view. Keeping this in view, we have additionally utilized the TMI dataset in our analysis of SST variability since it overcomes the problem of obstruction due to clouds (Wentz, 1998; Chelton *et al*., 2001; Harrison and Vecchi, 2001). Although the TMI SST is available for a relatively shorter period from December 1997 onward, it allows examination of SST variability

DOI: 10.1002/joc

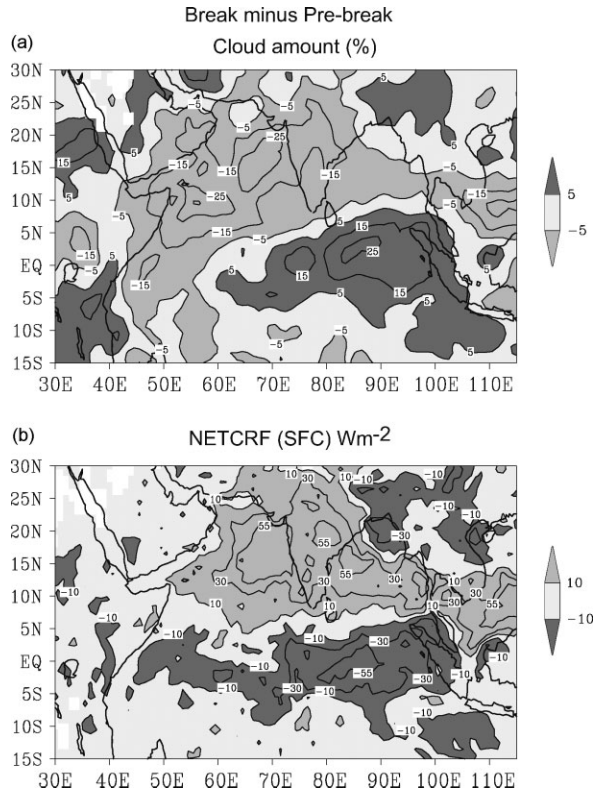

Figure 7. Difference maps ('break' minus 'pre-break') show the changes in **(a)** Total cloud amount (%) and **(b)** NETCRF (Wm^{-2}) at surface. The difference maps are composites constructed using the SRB dataset w.r.t. the prolonged monsoon breaks given in Table I.

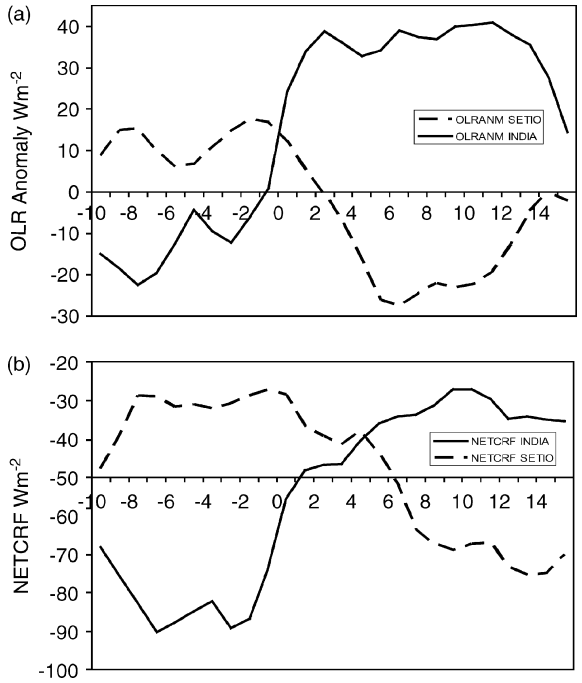

Figure 8. Composited time evolution of area-averaged OLR anomalies (Wm^{-2}) and NETCRF at the surface (Wm^{-2}) during monsoon-break transition. The composites are constructed on the basis of the prolonged monsoon breaks given in Table I. The solid line is for the Indian landmass (70 °E–85 °E; 16°N–28 °N) and the dashed line is for the SETIO (70 °E–105 °E; 10 °S–5 °N) **(a)** OLR anomalies from NOAA satellite **(b)** NETCRF at surface from SRB dataset.

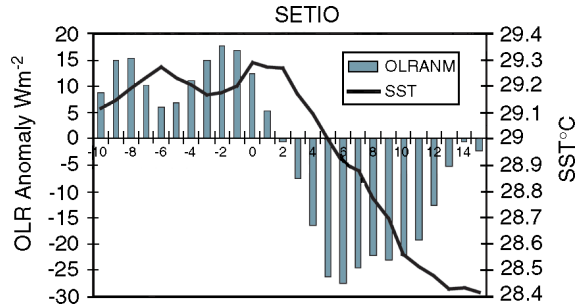

Figure 9. Composited time evolution of area-averaged OLR anomalies (Wm^{-2}) and SST (°C) in the SETIO region associated with the evolution of the prolonged monsoon breaks during 2002 and 2004 (Table I). The OLR anomalies are from NOAA satellite and the SST is based on the TMI dataset. This figure is available in colour online at www.interscience.wiley.com/ijoc

during the prolonged monsoon breaks that occurred during the summer seasons of 2002 and 2004 – which were two major monsoon droughts in the recent past. Also, the daily TMI SST has higher temporal representation of the intra-seasonal variability as compared to the weekly OISST.

First, we examine the daily evolution of OLR and SST from the TMI dataset for the SETIO region. Figure 9(a) shows the time variation of OLR anomalies over the SETIO composited w.r.t. the prolonged breaks during 2002 and 2004 (Table I). The positive OLR anomalies from Day (−10) to Day (+1) indicate lack of convection over the near-equatorial Indian Ocean. The appearance of negative OLR anomalies from Day (+2) onward indicate intensification of convection over the SETIO region following the initiation of 'monsoon break' over the Indian landmass. The time series of the TMI SST in the SETIO region (Figure 9(b)) shows a SST warming tendency from Day (−10) to Day (+1) – corresponding largely to the 'pre-break' phase when relatively cloud-free conditions prevail over the SETIO. It can be seen that the mean SST during the 'pre-break' phase is quite high (∼29.3 °C), suggesting that the lack of cloud cover over the SETIO acts to pre-condition the underlying ocean by allowing more solar insolation to warm the ocean surface. From Day (+2) onward, the SST variation over SETIO shows a cooling tendency associated with the enhancement of convection and cloud cover. The mean SST in the SETIO region averaged from Day (+2) to Day (+15) is about 28.6 °C. Thus, the typical change in SST in the SETIO from the 'pre-break' phase to the 'break' phase is around 0.7 °C. The decrease in the mean SST during the 'break' phase relative to the 'pre-break' phase is consistent with the reduction in solar insolation at the surface due to the increase in cloud cover over the SETIO.

Past studies have reported that the observed intra-seasonal variability of SST in the tropical Indian Ocean is predominantly driven by surface insolation anomalies associated with anomalous large-scale convection, with secondary contributions from the anomalies of latent

DOI: 10.1002/joc

and sensible heat flux across the Indian Ocean (e.g. Hendon and Glick, 1997; Shinoda *et al.*, 1998). Further model simulation experiments will be needed to accurately quantify the contributions of individual physical processes to the net surface heat flux variability and observed SST tendencies in the tropical Indian Ocean during break-monsoon transitions.

The spatial patterns of the SST difference ('break' minus 'pre-break') based on the OISST and TMI datasets are shown in Figure 10(a), (b). For the weekly OISST data, we have prepared SST composites during the 'pre-break' and 'break' phases based on the cases of prolonged breaks shown in Table I. Since we have considered breaks having duration longer than 2 weeks, the average of SST for the first and second weeks of the break period were taken as the 'break' phase. For the 'pre-break' phase, we have considered the average of SST for the two weeks preceding the break period. The SST difference ('break' minus 'pre-break') between the two phases is shown in Figure 10(a). The positive SST anomalies off the Somali Coast and in the southeastern and central Arabian Sea are consistent with decreased evaporation and weakened coastal upwelling due to weakening of the southwest monsoon flow (Ramesh and Krishnan, 2005) during the 'break' phase relative to the 'pre-break' phase. This warming tendency is brought out more prominently in the TMI SST (Figure 10(b)) as compared to that of the OISST. Cold anomalies can be seen in the northern Arabian Sea (north of 15 °N) off the Arabian Coast and northwest India. Examination of the wind field revealed intensification of southerlies over this region during the 'break' phase relative to the 'pre-break' phase (figure not shown). Our understanding suggests that the SST cooling (Figure 10) off the Arabian coast (north of 15 °N) involves not only changes in the net heat flux at the surface but also wind-induced changes in the ocean circulation. However, a detailed investigation of this issue will require a separate study. The point that is directly relevant to the present discussion is the occurrence of SST cooling in the equatorial and southern tropical Indian Ocean (Figure 10). Negative SST anomalies, in the range −0.5 °C to −0.9 °C, can be seen extending eastward from about 60 °E up to 95 °E. The cooling tendency in the SETIO is much more pronounced in the TMI dataset as compared to the OISST anomalies. The SST change of nearly −1.0 °C provides supporting evidence for the reduction in solar insolation at the surface over the SETIO region due to increase in cloud cover following the transition from the 'pre-break' phase to the 'break' phase.

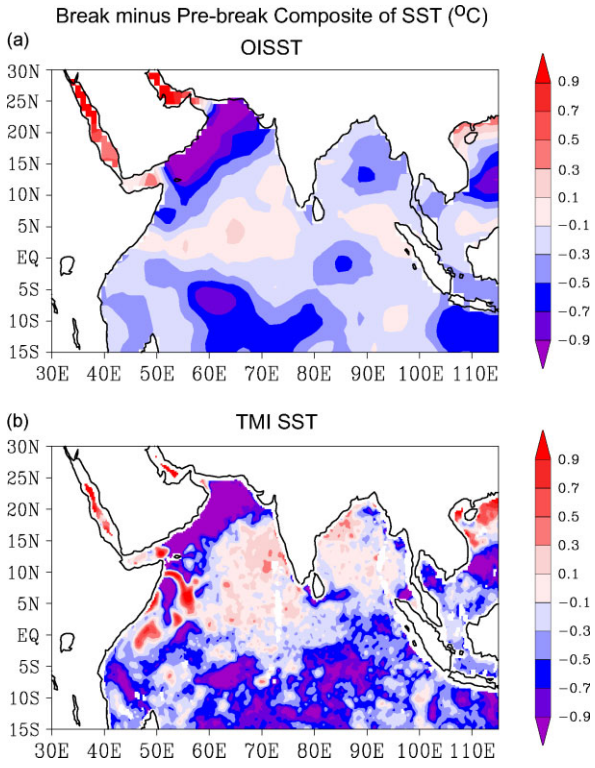

Figure 10. Spatial pattern shows the change in SST (°C) between the 'break' and 'pre-break' phase from the **(a)** weekly OISST **(b)** daily TMI dataset. The OISST composite is based on the all the prolonged breaks during 1982–2004 given in Table I. The TMI SST composite is based on the prolonged breaks during 2002 and 2004. This figure is available in colour online at www.interscience.wiley.com/ijoc

5. Discussions and concluding remarks

The implications of the CRF on the SST variability in the equatorial and southeastern tropical Indian Ocean are important in that they provide a physical basis for interpreting why monsoon breaks can sometimes prolong for more than 2–3 weeks, thereby leading to drought conditions over the Indian subcontinent. Anomalously warm SST in the SETIO associated with strong east–west SST gradients favour westerly winds along the equator, which enhance the moisture convergence and convective activity over the SETIO region (Krishnan *et al.*, 2006). GCM simulation experiments suggest that the enhancement of convective activity over the warm SETIO can induce anomalous subsidence over the Indian subcontinent and weaken the monsoon Hadley cell, thereby leading to deficient rainfall over India (Krishnan *et al.*, 2003).

It is seen from the present study that the scarcity of cloud cover over the SETIO during the 'pre-break' phase allows pre-conditioning of the equatorial Indian Ocean through increased solar insolation at the surface. During the 'pre-break' phase, the NETCRF at the surface is found to be typically about −30 Wm^{-2} with SSTs warmer than 29.3 °C in the SETIO region. Following the transition from the 'pre-break' to the 'break' phase, the convection over the Indian landmass is suppressed, while that over the equatorial Indian Ocean intensifies. Results from the present analysis indicate that the cloud amount over the SETIO can increase by nearly 25% following the transition to the 'break' phase. The NETCRF at the surface during 'break' phase over the SETIO is found to be around −60 Wm^{-2} (i.e. a change of about −30 Wm^{-2} from the 'pre-break' phase). SST measurements from the TMI indicate a cooling of about 0.7 °C in the SETIO associated with the reduction in solar insolation at the surface due to increase in cloud amounts following the monsoon-break transition.

DOI: 10.1002/joc

An important question is what sustains the anomalous convection over the SETIO during prolonged monsoon breaks? It must be pointed out that, despite the SST drop of about 0.7 °C during the monsoon-break transition, the mean SSTs in the SETIO during the 'break' phase were found to be as high as 28.6 °C. One possible explanation for the high SST is the ocean pre-conditioning during the 'pre-break' phase – wherein the lack of cloudiness over the SETIO allows increased solar insolation at the surface and warms the underlying ocean. Rajeevan (2001) suggested a similar mechanism for anomalous SST warming in the tropical Indian Ocean associated with the inter-annual variability of high clouds. In addition, Krishnan *et al*. (2006) have recently reported the possibility of a dynamical coupling between the southwest monsoon circulation and the thermocline depth variations in the eastern equatorial Indian Ocean on intra-seasonal timescales. In this dynamical feedback, anomalous westerly winds along the equator push warm water eastward, so as to deepen and warm the surface mixed layer in the eastern equatorial Indian Ocean and also maintain a strong east–west gradient of SST in the equatorial Indian Ocean. In turn, the warm and deep oceanic mixed layer drives anomalous convection in the atmosphere, which suppresses the monsoon Hadley circulation and reinforces the anomalous equatorial westerly winds through low-level convergence.

On the basis of the above discussions, it is inferred that the enhanced SST warming in the SETIO during the 'pre-break' phase as well as the mixed layer deepening by strong equatorial westerly winds significantly contribute to the maintenance of high SSTs (>28.5 °C) in the SETIO. It is realised that the relationship between the variability of SST and high clouds is rather complex for the Indian Ocean. Fu *et al*. (1990) suggested two types of relationships between deep convection, SST and surface convergence: (1) deep convection is enhanced in large regions where SST >28 °C, provided there is no strong surface divergence, (2) when the warmest SSTs in a region are less than about 28 °C, deep convection is significantly enhanced by strong surface wind convergence near the local maximum of SST (26°–28 °C). On the basis of the above points, it is deduced that the warm SST (>28.5 °C) during July 2002 and weak surface divergence over the SETIO were crucial in sustaining the enhanced convective activity over the region.

In summary, the present study has brought out the importance of cloud-radiative effects on the intraseasonal variability of SST in the SETIO region associated with the evolution of monsoon breaks. The findings lend credence to the occurrence of significant SST warming in the SETIO during the 'pre-break' phase, in association with increased surface solar insolation under relatively cloud-free conditions over the region. It is hypothesised that this pre-conditioning of the SETIO during the 'pre-break' phase is important for sustaining high values of mean SST (>28.5 °C) during prolonged monsoon breaks. These results could have likely implications on foreshadowing the monsoonal rains on timescales of days to weeks. In a more recent study, Veechi and Harrison (2002) have suggested that SST variations in the Bay of Bengal can be useful precursors of an ensuing monsoon break. Since the suppression of convection over the SETIO and the associated SST warming in the region appear nearly 7–10 days prior to the initiation of a monsoon break over India, efforts to monitor the coupled interactions in the tropical Indian Ocean would greatly help in tracking the evolution of monsoon breaks. The analysis presented here has been mostly explorative in nature; it is our future plan to carry out coupled model experiments to better quantify the details of the ocean-atmosphere coupling during monsoon-break transitions.

Acknowledgements

This research work was funded by the DOD/INDOMOD-SATCORE project ISP1.5, Department of Ocean Development, Government of India. We thank the Director, Indian Institute of Tropical Meteorology, for providing the necessary infrastructural facilities to carry out this research work. We are grateful to the anonymous reviewers for providing valuable comments. The data support from Remote Sensing Systems, CA, USA, NASA Langley Research Center Atmospheric Sciences Data Center, National Center for Environmental Prediction (NCEP), USA, Climate Diagnostic Center (CDC), USA – is gratefully acknowleged.

References

Annamalai H, Slingo JM. 2001. Active/Break cycles: diagnosis of the intraseasonal variability of the Asian Summer Monsoon. *Climate Dynamics* **18**: 85–102.

Bhat GS, Gadgil S, Hareesh Kumar PV, Kalsi SR, Madhusoodanan P, Murthy VSN, Prasada Rao CVK, Ramesh Babu V, Rao LVG, Rao RR, Ravichandran M, Reddy KG, Sanjeeva Rao P, Sengupta D, Sikka DR, Swain J, Vinayachandran PN. 2001. BOBMEX: the bay of bengal monsoon experiment. *Bulletin of the American Meteorological Society* **82**: 2217–2243.

Chelton DB, Esbensen SK, Schlax MG, Thum N, Freilich MH, Wentz FJ, Gentemann CL, McPhaden MJ, Schopf PS. 2001. Observations of coupling between surface wind stress and sea surface temperature in the eastern tropical Pacific. *Journal of Climate* **14**: 1479–1498.

Collins VD, Valero FPJ, Flatau PJ, Lubin D, Grassl H, Pilewskie P. 1996. Radiative effects of convection in the tropical Pacific. *Journal of Geophysical Research* **101**: 14,999–15,012.

Fasullo J. 2005. Atmospheric hydrology of the anomalous 2002 Indian summer monsoon. *Monthly Weather Review* **133**: 2996–3014.

Fu X, Wang B. 2004. Differences of boreal-summer intraseasonal oscillations simulated in an atmosphere-ocean coupled model and an atmosphere-only model. *Journal of Climate* **17**: 1263–1271.

Fu R, Del Genio AD, Rossow WB. 1990. Behavior of deep convective clouds in the tropical Pacific deduced from ISCCP radiances. *Journal of Climate* **3**: 1129–1152.

Fu R, Liu WT, Dickinson RE. 1996. Response of tropical clouds to the interannual variation of sea surface temperature. *Journal of Climate* **9**: 616–634.

Fu X, Wang B, Li T, McCreary JP. 2003. Coupling between northward propagating, intraseasonal oscillations and sea-surface temperature in the Indian Ocean. *Journal of the Atmospheric Sciences* **15**: 1733–1753.

Gadgil S, Rajeevan M, Nanjundiah R. 2005. Monsoon prediction- why yet another failure? *Current Science* **88**: 1389–1400.

Goswami BN. 2005. South Asian monsoon. In *Intraseasonal Variability of the Atmosphere-Ocean Climate System*, Lau WKM, Waliser DE (eds). Springer: Heidelberg; 19–61, Chapter 2.

DOI: 10.1002/joc

Harrison DE, Vecchi GA. 2001. January 1999 Indian Ocean cooling event. *Geophysical Research Letters* **28**: 3717–3720.

Harrison EF, Minnis P, Barkstrom BR, Ramanthan V, Cess RD, Gibson GG. 1990. Seasonal variation of cloud radiative forcing derived from the Earth Radiation Budget Experiment. *Journal of Geophysical Research* **95**: 18 687–18 703.

Hartmann DL, Michelsen ML. 1989. Intraseasonal periodicities in Indian rainfall. *Journal of the Atmospheric Sciences* **46**: 2838–2862.

Hartmann DL, Ockert-Bell ME, Michelson ML. 1992. The effect of cloud type on earth's energy balance: global analysis. *Journal of Climate* **5**: 1281–1304.

Hendon HH, Glick J. 1997. Intraseasonal air-sea interactions in the tropical Indian and Pacific Oceans. *Journal of Climate* **10**: 647–661.

Kiehl JT. 1994. On the observed near cancellation between longwave and shortwave cloud forcing in tropical regions. *Journal of Climate* **7**: 559–565.

Kiehl JT, Ramanathan V. 1990. Comparison of cloud forcing derived from the Earth Radiation Budget Experiment with that simulated by the NCAR community climate model. *Journal of Geophysical Research* **95**: 11679–11698.

Krishnamurti TN, Bhalme HN. 1976. Oscillations of a monsoon system. Part I: Observational aspects. *Journal of the Atmospheric Sciences* **33**: 1937–1954.

Krishnamurti TN, Subrahmanyam D. 1982. The 30–50 day mode at 850 mb during MONEX. *Journal of the Atmospheric Sciences* **39**: 2088–2095.

Krishnamurti TN, Oosterhof DK, Mehta AV. 1988. Air-sea interaction on the timescale of 30 to 50 days. *Journal of the Atmospheric Sciences* **45**: 1304–1322.

Krishnan R, Zhang C, Sugi M. 2000. Dynamics of Breaks in the Indian summer monsoon. *Journal of the Atmospheric Sciences* **57**: 1354–1372.

Krishnan R, Mujumdar M, Vaidya V, Ramesh KV, Satyan V. 2003. The abnormal Indian summer monsoon of 2000. *Journal of Climate* **16**: 1177–1194.

Krishnan R, Ramesh KV, Samala BK, Meyers G, Slingo JM, Fennessy MJ. 2006. Indian Ocean-monsoon coupled interactions and impending monsoon droughts. *Geophysical Research Letters* **33**: L08711, DOI: 10.1029/2006GL025811.

Kumar V, Krishnan R. 2005. On the association between the Indian summer monsoon and the tropical cyclone activity over northwest Pacific. *Current Science* **88**(4): 602–612.

Lau KM, Chan PH. 1986. Aspects of the 40–50 day oscillation during the northern summer as inferred from outgoing longwave radiation. *Monthly Weather Review* **114**: 1354–1367.

Rajeevan M. 2001. Interactions among deep convection, sea surface temperature and radiation in the Asian monsoon region. *Mausam* **52**: 83–96.

Rajeevan M, Srinivasan J. 2000. Net cloud radiative forcing at the top of the atmosphere in the Asian Monsoon region. *Journal of Climate* **13**: 650–657.

Ramamurthy K. 1969. Some aspects of the break in Indian southwest monsoon during july and august. *India Meteorological Department Forecasting Manual* **No. IV-18.3**, Poona, India; 57.

Ramanathan V, Cess RD, Harrison EF, Minnis P, Barkstrom BR, Ahmed E, Hartmann D. 1989. Radiative cloud forcing and climate: Results from the Earth Radiation Budget Experiment. *Science* **243**: 57–63.

Ramesh KV, Krishnan R. 2005. Coupling of mixed layer processes and thermocline variations in the Arabian Sea. *Journal of Geophysical Research* **110**: C5, C05005, DOI: 10.1029/2004JC002515.

Rao YP. 1976. Southwest monsoon India Meteorological Department. *Meteorological Monograph Synoptic Meteorology* **No. 1/1976**, Delhi; 367.

Rao RR. 1987. The observed variability of the cooling and deepening of the mixed layer in the central Arabian Sea during Monsoon-77. *Mausam* **38**: 43–48.

Rossow WB, Schiffer RA. 1999. Advances in understanding clouds from ISCCP. *Bulletin of the American Meteorological Society* **80**: 2261–2288.

Saith N, Slingo JM. 2006. The role of the Madden Julian Oscillation in the Indian drought of 2002. *International Journal of Climatology* **26**: 1361–1378.

Sathiyamoorthy V, Pal PK, Joshi PC. 2004. Influence of the upper-tropospheric wind shear upon cloud radiative forcing in the Asian monsoon region. *Journal of Climate* **17**: 2725–2735.

Sengupta D, Ravichandran M. 2001. Oscillations of Bay of Bengal sea surface temperature during the 1998 summer monsoon. *Geophysical Research Letters* **28**: 2033–2036.

Sengupta D, Goswami BN, Senan R. 2001. Coherent intraseasonal oscillations of ocean and atmosphere during the Asian Summer Monsoon. *Geophysical Research Letters* **28**: 4127–4130.

Shinoda T, Hendon HH, Glick J. 1998. Intraseasonal variability of surface fluxes and sea surface temperature in the tropical western Pacific and Indian Oceans. *Journal of Climate* **7**: 929–948.

Sikka DR. 1999. Monsoon drought in India. Joint COLA/CARE Tech. Rep. No. **2**. Center for Ocean-Land-Atmosphere Studies and Center for the Application of Research on the Environment; COLA, Calverton, MD, USA, 93.

Sikka DR, Gadgil S. 1980. On the maximum cloud zone and the ITCZ over Indian longitudes during the southwest monsoon. *Monthly Weather Review* **108**: 1840–1853.

Singh SV, Kripalani RH. 1985. South to north progression of rainfall anomalies across India during summer monsoon season. *PAGEOPH* **123**: 624–637.

Stephens GL, Greenwald TJ. 1991. The Earth's radiation budget and its relation to atmospheric hydrology. Part 2. Observations of cloud effects. *Journal of Geophysical Research* **96**: 15325–15340.

Veechi GA, Harrison DE. 2002. Monsoon breaks and subseasonal sea surface temperature variability in the Bay of Bengal. *Journal of Climate* **15**: 1485–1493.

Waliser DE. 2005. Predictability and forecasting tropical intraseasonal variability. In *Intraseasonal Variability of the Atmosphere-Ocean Climate System*, Lau WKM, Waliser DE (eds). Springer: Heidelberg; 401–434.

Wentz FJ. 1998. Algorithm theoretical basis document: AMSR Ocean Algorithm. Remote Sensing Systems Tech Report **110398**, Remote Sensing Systems: Santa Rosa, CA; 65.

Wielicki BA, Barkstrom BR, Harrison EF, Lee RB III, Smith GL, Cooper JE. 1996. Clouds and the Earth's Radiant Energy System (CERES): an earth observing system experiment. *Bulletin of the American Meteorological Society* **77**: 853–868.

Woolnough SJ, Slingo JM, Hoskins BJ. 2000. The relationship between convection and sea surface temperature on intraseasonal timescales. *Journal of Climate* **13**: 2086–2104.

Yasunari T. 1979. Cloudiness fluctuations associated with the Northern Hemisphere summer monsoon. *Journal of the Meteorological Society of Japan* **57**: 227–242.

Zhang YC, Rossow WB, Lacis AA, Oinas V, Mishchenko MI. 2004. Calculation of radiative fluxes from the surface to top of atmosphere based on ISCCP and other global data sets: Refinements of the radiative transfer model and the input data. *Journal of Geophysical Research* **109**: D19105, DOI: 10.1029/2003JD004457.